

# Application of Artificial Intelligence in Single Point Incremental Forming for Surface Roughness Prediction

*Ranjeet Prasad<sup>1</sup>, Manish Oraon<sup>2\*</sup>, and Vinay Sharma<sup>3</sup>*

<sup>1</sup>Research Scholar, Department of Production and Industrial Engineering, Birla Institute of Technology, Mesra, India

<sup>2,3</sup>Faculty, Department of Production and Industrial Engineering, Birla Institute of Technology, Mesra, India

## *Abstract*

*Keywords: SPIF, Input Parameters, Surface Roughness, ANOVA, ANN*

*\*Author for Correspondence* E-mail: [moraon@bitmesra.ac.in](mailto:moraon@bitmesra.ac.in),

## INTRODUCTION

In recent years, an effort has made the manufacturing industry to minimize the processing period and cost of production. The need of customized part, model, and production of small batch enunciate the techniques like rapid prototyping, 3D printing etc. These advanced technologies turn the raw materials into finished part in less time and minimum effort [1]. Accordingly, an advanced technique, known as Incremental sheet metal forming (ISMF), is developed to accelerate the forming industries. The flexible processing of ISMF comprises higher complexity therefore an attention towards calibration of the process is required [2]. The spring-back effect was merely investigated as it is not observed excessively in small part formation, but it was tried to simulate through different techniques [3-4]. The construction of computational systems and algorithms is a basic science of artificial intelligence (AI) that can perform a variety of tasks such as learning, interpretation reasoning, decision making etc. [5-6]. In Manufacturing, AI has important applications in different areas such as process planning, quality control, predictive maintenance, optimization, logistic, etc. [7]. The technological principle of SPIF involves clamping the blank from its edges and progressively deforming it using a single hemispherical end rod as per input commands in computer numerical control (CNC) based machine. Researchers have proposed several approaches to SPIF, however strong results are still awaited. The main limitations of SPIF, such as longer process time, sheet thinning, and limited geometrical accuracy, hinder its wider industrial application [8]. Extensive investigations concentrated on the maximum forming of thin sheet of metal without failure and their optimization in ISMF. Industrial research primarily targets the geometric precision of forming parts, both at the macroscopic levels. An experimental-statistical analysis is conducted on calamine brass Cu67Zn33 to examine the roughness profile of the product. Earlier investigations has indicated that the deformation rate is important factor in the SPIF process [9-12]. Preliminary studies of SPIF on SPCC steel [13] reveals that the finished parts exhibited spring back and dimensional inaccuracy when SPIF is done with varying wall angles that results a large-scale waviness in the formed part [14]. By decreasing the vertical step size, the surfaces transformed from wavy to strictly rough [15]. The non-contacted surface roughness measurements system was utilized to measure sectional microstructure, and thickness distribution in the SPIF of AL3003 (H14) at higher tool feed rate and higher tool rotational speeds [16]. Experimental campaigns were analysed on AA7075 alloy to draw conclusions regarding the influence of the said parameters [17-18]. The medical implants were successfully formed through SPIF [19]. It was observed that the reducing friction and achieving reduced level of roughness on the punch surface improved the interior surface of titanium sheets. The effects of tool diameter, along with other process parameters were investigated during SPIF on various Indian standard metals such as steel, stainless steel, and aluminium to analyse the surface roughness and microstructural transformation. It is

observed that a larger tool end diameter of hemispherical end tool and higher spindle speed improved the desired goals [20]. The formability of stainless steel SS304 grade through SPIF was investigated by considering variations in tool end along with few process variables. Statistical analysis showed that vertical size increment i.e. step-depth size increment contributed significantly to surface roughness [21]. Further the gradient boosting regression tree (GBRT) is used to correlate the functional variables of SPIF on the output response for Al/SUS bimetal sheet. The authors reported severe cracks when SPIF was done with 10 mm tool end diameter while the refinement in the surface roughness was noticed with 20 mm tool end diameter and small step size of 0.15 mm [22]. Overall, these studies and investigations highlight the various aspects, parameters, and challenges involved in SPIF, keeping all these finding in mind, the artificial neural network (ANN) model is introduced in SPIF to predict the surface quality of formed part which is a prime concern.

## SPIF INVESTIGATION

Taguchi-based optimization offers advantages over conventional optimization practices with a minimum number of experiments [23]. Unlike traditional methods, Taguchi optimization is more cost-effective. However, to address the limitation of optimizing only one characteristic, several modifications have been suggested [24]. These modifications aim to extend the Taguchi method to handle multi-objective problems, but these modifications increase the computational complexity of the optimization process. In the context of multi-objective optimization, a simple modification has been proposed. This modification, described in [25], introduces a multi-objective for individual trial of the Orthogonal Array (OA). By using these membership functions, the multi-performance objectives can be considered simultaneously during the optimization process. This modified approach enables Taguchi-based optimization to handle multi-objective problems without significantly increasing computational complexity. It provides a more comprehensive and efficient way to optimize multiple performance characteristics simultaneously, making it a valuable tool in engineering and optimization applications.

### SPIF Experiments

The SPIF experiments is conducted on CNC vertical machine centre (Model: DT-110, Mikrotool Pvt. Ltd., Singapore) place in the modern manufacturing laboratory of production and industrial engineering department, BIT, Mesra. A dedicated SPIF fixture is designed and fixed it over the CNC's table. The lower and higher value of the SPIF parameters domains i.e. step-depth size ( $\Delta z$ ) in mm, feed rate ( $f$ ) in mm/min, spindle speed ( $R$ ) in RPM, wall angle ( $\theta$ ) in degree, sheet thickness ( $T$ ) in mm, and density of lubricant ( $L$ ) in  $\text{kg/m}^3$  are taken. The numeric values of considered input parameters for SPIF experiment is tabulated in Table 1. The Cu-Zn alloy is taken as metal sheet and a square pyramid shape of given dimensions is formed in each test sample with the prescribed tool trajectory as in Fig. 1.

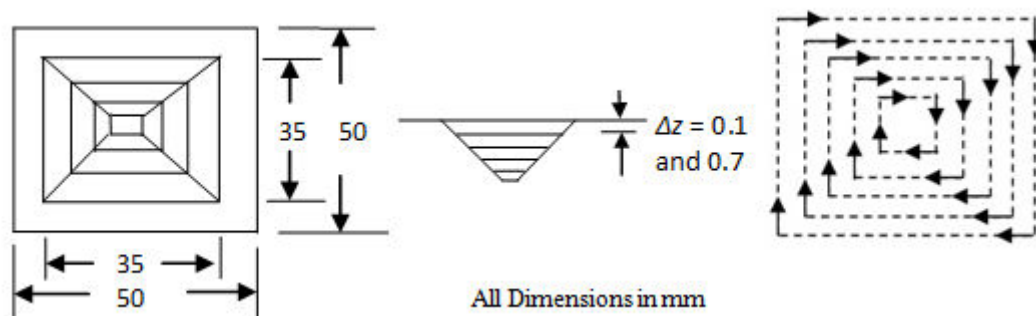


*Fig. 1: Proposed Square Pyramid Shape and Toolpath for Forming.*

The test sample is prepared by cutting 5mm\*5mm from individual square pyramid for measuring the surface roughness measurement (See Fig. 2). Across the direction of tool movement as expected the waviness observed in the formed part due to continuous change in successive depth. The surface roughness of the cut sample of each experiment is measured in the magnification of 100X through atomic force measurement machine (AFM) (Model: NT-MDT, Solver-4) which is available in the central instrumentation facility-1 (CIF-1), BIT, Mesra, India.



**Fig. 2:** AFM (Model: NT-MDT) Solver-4 Used in Surface Roughness Measurement.

The test sample piece is placed in the machine in such a way that optical probe scans the sample across the tool feed mark (due maximum surface roughness occur due to waviness). The optical probe scanned approximately 65000 grits in one pass and generated a 3D microscopic image along with average surface roughness ( $Ra$ ), average heights of top ten peaks ( $Ry$ ), and root mean square roughness ( $Rq$ ). All the roughness values are measured in micron ( $\mu$ ) level. Only average surface roughness  $Ra$  is considered in the present study. The sample, cut section and AFM microscopic image of individual samples is presented in Fig. 3. The experiment set with varying level of input parameters along with measured  $Ra$  is tabulated in Table 1.

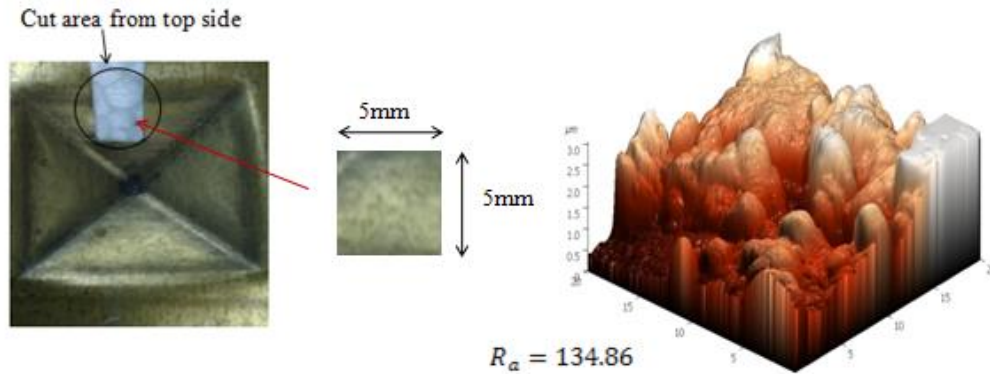


**Fig. 3:** Sample Cut for AFM and Microscopic Image of a Sample

### Statistical Analysis for $Ra$

In the present investigation, the significant input parameters on the output response, specifically the surface roughness ( $Ra$ ) are being analyzed using statistical methods. The software used for this analysis is MINITAB version 17.0.1, a popular tool for statistical analysis. In this case, it is used to assess how the input variables affect the output factor  $Ra$ . The significance level chosen for the analysis of variance ANOVA is 95% confidence. This means that there is a 95% probability that any observed differences in the output response ( $Ra$ ) are not due to random chance but are instead influenced by the variations in the input parameters. The significance level is often denoted by the symbol alpha ( $\alpha$ ), and in this case, it is set to 0.05 (5%). The lower  $Ra$ -value shows the improved surface finish of the product therefore ‘smaller is better’ approach is made during ANOVA test. The equation for ‘smaller is better’ is expressed by equation (1).

$$S/N_{(smaller\ is\ better)} = -10\log -10\log_{10}\left(SUM\left(\frac{Y^2}{n}\right)\right) \quad (1)$$

**Table 1:** EXPERIMENT SET AS PER ORTHOGONAL ARRAY  $L_{16}$  ALONG WITH MEASURED  $Ra$ .

Exp. No.	$\Delta z$ ( $10^{-1}$ )	$F$ ( $10^1$ )	$R$ ( $10^2$ )	$T$ ( $10^{-1}$ )	$\theta$	$L$ ( $10^{-1}$ )	$Ra$
1	1	2	5	2	15	1.5	62.951

2	1	2	5	4	45	4.9	104.863
3	1	2	20	4	15	4.9	58.29
4	1	2	20	2	45	1.5	102.943
5	1	10	5	4	15	4.9	67.6545
6	1	10	5	2	45	1.5	100.514
7	1	10	20	2	15	1.5	51.8449
8	1	10	20	4	45	4.9	107.392
9	7	2	5	4	15	4.9	89.637
10	7	2	5	2	45	1.5	86.358
11	7	2	20	2	15	1.5	130.65
12	7	2	20	4	45	4.9	144.369
13	7	10	5	2	15	1.5	74.845
14	7	10	5	4	45	4.9	152.597
15	7	10	20	4	15	4.9	86.102
16	7	10	20	2	45	1.5	151.637

### Artificial Neural Network Modeling

In manufacturing, the variation in the outputs is very common for repeated experiments. The inconsistency in the output response may arise from the full proofing of the conducted experiments. Moreover, the variation in the input parameters magnitude enhanced the estimation of conducted experiments. To correlate the results, the prediction of output needs to be analyzed in such a manner so that the error on the product should be minimized [26]. Artificial Intelligence (AI) is a widely utilized tool in many sectors and set a benchmark [27-29]. Artificial Neural Network (ANN) is a module of AI utilized as predictor tool in various sectors such as manufacturing processes, healthcare, finance, sports, etc. to model the nonlinear functions into a reliable output [30-31]. In the continuing SPIF investigation ANN estimated that the deformation velocity rate, element size, and mass scaling as 16.49m/s, 1mm\*1mm, and 19.01 respectively to minimize pillow effect [32]. With the insight knowledge of ANN, the present investigation is done on MATLAB version 7.10.0.499 (Math works Inc., U.S.A) where Levenberg- Marquardt algorithm is utilized. The 6-6-1 network topology as shown in Fig. 4 is developed. The experimental numeric codes of input parameters and the measured output response i.e.  $R_a$  is taken as inputs for the prediction of  $R_a$ .

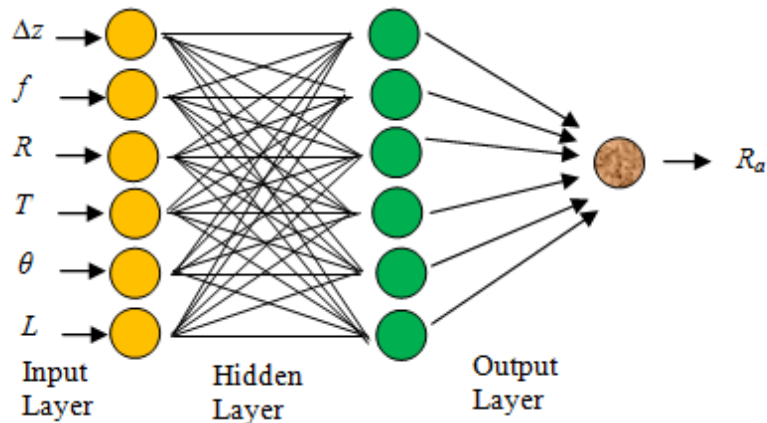


**Fig. 4:** ANN Network Architecture 6-6-1 for  $R_a$

According to Fig. 4, net input to unit 'k' in the hidden layer for single layer feed forward network is expressed in equation (2),

$$net\_hidden = \sum_{j=1}^j wt_{j,k}i_j + bs_k \quad (2)$$

Where  $wt_{j,k}$  is the weight,  $bs_k$  are the biases, and  $i_j$  is the inputs value. Now, the net input (for unit z) received is expressed in equation (3),

$$net\_output = \sum_{k=1}^k v_{k,z}h_k + c_z \quad (3)$$

Where  $v_{k,j}$  is the weight,  $c_z$  is the biases, and  $h_k$  is the outputs value at hidden nodes. After equating equations (2) and (3), the output at hidden and output nodes can be written as. equation (4) and equation (5) are the net information communicated to next layer for further analysis.

$$h_k = f(net\_hidden) \quad (4)$$

$$o_z = f(net\_output) = R_a \quad (5)$$

Where  $h_k$  is the net information transferred from input layer to hidden layer whereas  $o_z$  is the net information transferred to output layer.

The variety of ANN model is tested to get the best functional model for the prediction of  $Ra$  of SPIFed part. The ANN architecture is classified into three sections as shown in Table 3. In section 1, the transfer function TANSIG and at output layer, PURELIN transfer function is used. Similarly, section 2 is modeled by introducing LOGSIG at hidden layer whereas PURELIN transfer function at output layer and in the last section e.g. section 3, PURELIN transfer function in introduced at both hidden and output layers respectively. All the models are run by varying neurons e.g. 10, 11, and 12 neurons to find record the behavioral change of the ANN model. The feed forward backpropagation neural network (FFBP) in which Levenberg Marquardt (LM) training algorithm and LERNGDM learning rate are adopted for simulation of all the NN models. The mean square error (MSE) is the target which is further considered to confirm the reliability of the NN model.

## RESULT AND DISCUSSION

The statistical analysis is done with 95% confidence level in which the probability factor (P) must be less than 0.05 shows the significance of individual input parameters. It is found step depth ( $\Delta z$ ) and forming angle ( $\theta$ ) are the significant process parameters for the  $Ra$ -value in the SPIF of Cu67Zn33 alloy. Analysis of variance (ANOVA) results shows graphically in Fig. 5 where slopes of individual input parameters are drawn. The low level of input variables  $\Delta z - f - R - T - L$  whereas  $\theta=45^\circ$  must be set in the SPIF of Cu67Zn33 alloy. Table 2 indicated that the step depth  $\Delta z$  (P=0.007) and wall angle  $\theta$  (P= 0.001) are the significant.

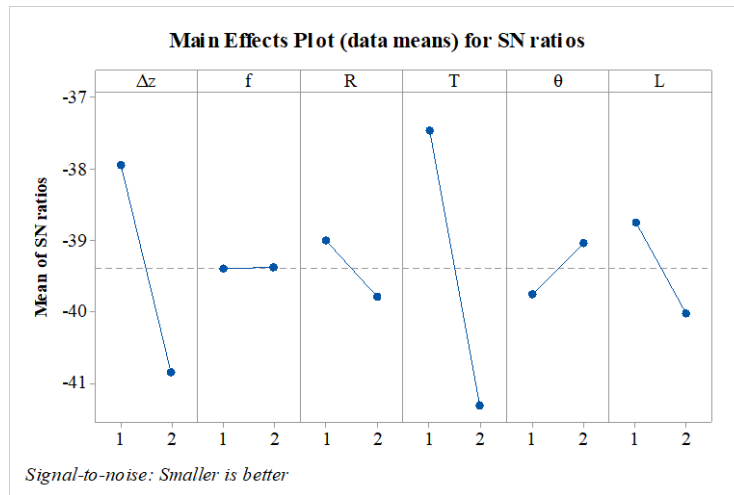


**Fig. 5: Main Effect Plot of Individual Input Parameters**

**Table 2: SIGNIFICANCE OF INPUT PARAMETERS FOR  $R_a$  SHOWN IN ANOVA.**

Source	DF	Seq SS	Adj SS	F	P	Significance
$\Delta z$	1	33.739	33.7493	11.85	0.007	Yes
$f$	1	0.003	0.0027	0.00	0.976	No
$R$	1	2.506	2.5063	0.88	0.373	No
$\theta$	1	59.226	59.2263	20.79	0.001	Yes
$T$	1	2.006	2.0061	0.70	0.423	No
$L$	1	6.462	6.4623	2.27	0.166	No
Residual Error	9	25.641	25.6409			
Total	15	129.594				

In ANN modeling, the input data are divided into 70% for training, 15% for testing and validation. The maximum numbers of iteration (first activated) and sufficient accuracy i.e. two stopping criteria is adopted during training of NN models. The network architecture generated by NN tool for the best possible solution is shown in Fig. 6.

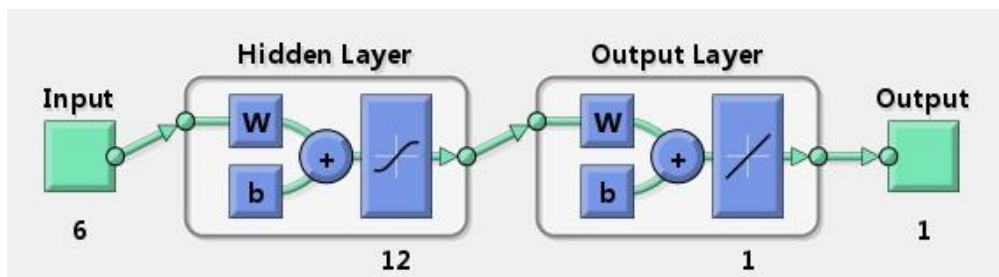


**Fig. 6: Main Effect Plot of Individual Input Parameters**

The  $R_a$ -value is predicted by using various ANN models in which neurons at hidden layer and type of transfer functions were varied. The training stopped at fifth iterations (first activated) with the value of 250.2109. The overall regression plot i.e. training, testing, and validation for the best possible NN solution are shown in Fig. 7. It seems that the input data for NN is to track the targets reasonably well.

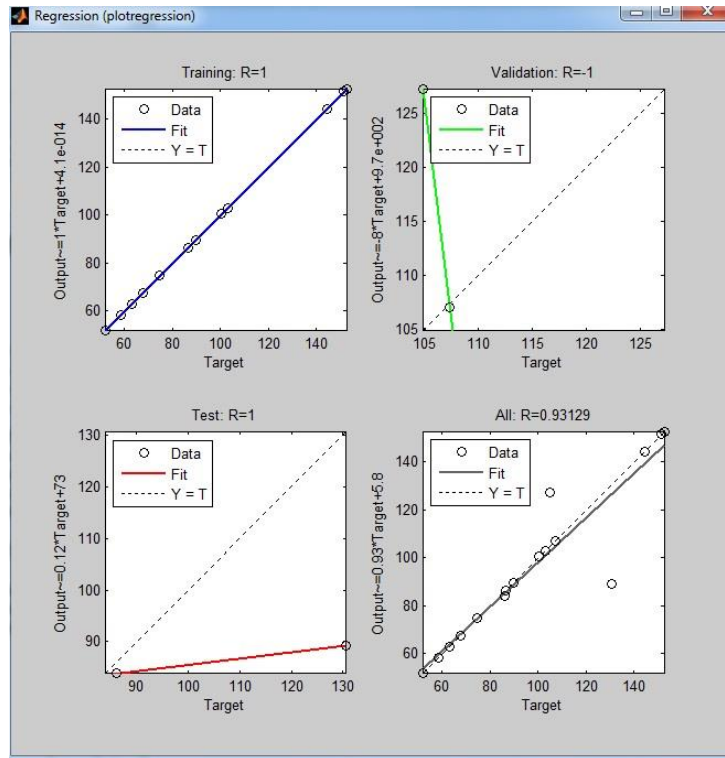


**Fig. 7: BPNN Regression Plot for Best NN Model**

Table 3 indicates the coefficient of correlation (CoC) for all the tested models are quite acceptable since the CoC for training, testing, and validation are more than 0.85 in most of the cases. To select the best ANN, the optimized CoC of 0.93219 with MSE of -5.34517 are reported in 6-12-1 NN where TANSIG at hidden layer and PURELIN at output layer. The training, testing and validation CoC's are reported as 1 for all and 0.93129 is overall CoC for the same NN model (Section 1 in Table 3). It seems that the input data for NN modeling tracked the targets reasonably well.

**Table 3: RESULTS OF ANN FOR TARGETED  $R_a$  AND PREDICTED  $R_a$  WITH MEAN SQUARE ERROR.**

	Hidden layer neuron	Transfer function		$R^2$				MSE
		Layer 1	Layer 2	Training	Testing	Validation	All	
<b>Section 1</b>	Source	TANSIG	PURELIN					
	10			1	0.99492	0.98472	0.91622	-4.02081
	11			1	0.93854	0.99923	0.92942	-3.04E-06
	<b>12</b>			<b>1</b>	<b>1</b>	<b>1</b>	<b>0.93129</b>	<b>-1.37</b>
<b>Section 2</b>		LOGSIG	PURELIN					
	10			1	0.92499	0.40038	0.80506	-2.87172
	11			1	0.86778	0.999981	0.77228	21.92478
	12			1	0.99612	0.88539	0.83074	1.090619
<b>Section 3</b>		PURELIN	PURELIN					
	10			0.91219	0.99238	0.98255	0.82366	-6.90808
	11			0.92581	0.9993	0.96385	0.84981	1.249844
	12			0.96902	0.99541	0.94326	0.85703	5.609581

The correlation between predicted and actual response indicated by  $R_a$  -value which is in the range of 0 to 1.0. In the study, the lowest MSE value is observed for optimum ANN network. The combination of TANSIG with PURELIN in ANN is found most efficient than other combinations to get accurate

results. Table 4 shows the comparative LM algorithm performance which is compared with measure  $R_a$  with MSE.

**Table 4: COMPARATIVE  $R_a$  ALONG WITH MSE FOR BEST FFBP MODEL**

Exp. No.	Experimental $R_a$ ( $\mu$ )	Predicted $R_a$ ( $\mu$ )	Error (MSE)
1	62.951	62.951	0
2	104.863	127.2294	0
3	58.29	58.29	0
4	102.943	102.943	0
5	67.6545	67.6545	0
6	100.514	100.514	0
7	51.8449	51.8449	0
8	107.392	106.9841	0
9	89.637	89.637	-2.13E-14
10	86.358	86.358	-22.3664
11	130.65	89.30209	-2.84E-14
12	144.369	144.369	1.42E-14
13	74.845	74.845	1.42E-14
14	152.597	152.597	0
15	86.102	83.91287	-1.42E-14
16	151.637	151.637	0.40794

## CONCLUSIONS

The surface roughness of the end part is examined and simultaneously analyzed the significance of input parameters. The prediction model is developed through ANN and feed forward back propagation method is utilized to enlighten the feasibility of AI tool in manufacturing processes. A few concluding points of the present study are mentioned below.

- The  $R_a$  -value of calamine brass can be improved by conduction SPIF at low step depth  $\Delta z$  along with greater wall angle.
- The optimum design for SPIF corresponds to  $\Delta z=0.1\text{mm}$ ,  $f=100\text{mm/min}$ ,  $R=500$ ,  $T=0.2\text{mm}$ ,  $\theta=45^\circ$ , and  $L=15\text{Kg/m}^3$ .
- The 6-12-1 model with TANSIG at hidden layer and PURELIN at output is found appropriate for predicting  $R_a$ .
- The CoC of 0.94855 is noticed resembles good agreement between input and output.
- ANN results found good agreement with experimental data where CoC found 0.94855 with MSE of -5.34517.

It is inferred that the output response is efficiently predicted through ANN. The benefit of using ANN included economic, approximate predictability, short simulation time which makes it a promising modelling tool. ANN could benefit industries in research and development activities.

## ACKNOWLEDGMENTS

The authors acknowledge the department of production and industrial engineering, BIT Mesra for their support and gratitude to FIST-II project sponsored by the department of science and technology, GOI.

## REFERENCES

- [1] Porteus EL. Optimal Lot Sizing, Process Quality Improvement and Setup Cost Reduction. *Oper Res.* 1986;34(1):137-144.
- [2] Jeswiet J, Micari F, Hirt G, Bramley A, Duflou J, Allwood J. Asymmetric single point incremental forming of sheet metal. *CIRP Ann - Manuf Technol.* 2005;54(2):88-114.
- [3] Gomes C, Onipede O, Lovell M. Investigation of springback in high strength anisotropic steels. *J Mater Process Technol.* 2005;159(1):91-98.
- [4] Xu WL, Ma CH, Li CH, Feng WJ. Sensitive factors in springback simulation for sheet metal forming. *J Mater Process Technol.* 2004;151(1-3):217-222.
- [5] Leo Kumar SP. State of The Art-Intense Review on Artificial Intelligence Systems Application in Process Planning and Manufacturing. *Eng Appl Artif Intell.* 2017;65:294-329.
- [6] Pham DT, Afify AA. Machine-learning techniques and their applications in manufacturing. *Proc Inst Mech Eng Part B J Eng Manuf.* 2005;219(5):395-412.
- [7] Fahle S, Prinz C, Kuhlenkötter B. Systematic review on machine learning (ML) methods for manufacturing processes – Identifying artificial intelligence (AI) methods for field application. *Procedia CIRP.* 2020;93:413-418.
- [8] Shim MS, Park JJ. The formability of aluminum sheet in incremental forming. *J Mater Process Technol.* 2001;113(1-3):654-658.
- [9] Ambrogio G, Cozza V, Filice L, Micari F. An analytical model for improving precision in single point incremental forming. *J Mater Process Technol.* 2007;191(1-3):92-95.
- [10] Bahloul R, Arfa H, Belhadjsalah H. A study on optimal design of process parameters in single point incremental forming of sheet metal by combining Box-Behnken design of experiments, response surface methods and genetic algorithms. *Int J Adv Manuf Technol.* 2014;74(1-4):163-185.
- [11] Oraon M, Sharma V. Predicting force in single point incremental forming by using artificial neural network. *Int J Eng Trans A Basics.* 2018;31(1):88-95.
- [12] Park JJ, Kim YH. Fundamental studies on the incremental sheet metal forming technique. *J Mater Process Technol.* 2003;140(1-3 SPEC.):447-453.
- [13] Pohlak M, Majak J, Küttner R. Manufacturability and limitations in incremental sheet forming. *Est J Eng.* 2007;13(2):129. doi:10.3176/eng.2007.2.06
- [14] Luo Y, He K, Du R. A new sheet metal forming system based on incremental punching, part 2: Machine building and experiment results. *Int J Adv Manuf Technol.* 2010;51(5-8):493-506.
- [15] Hagan E, Jeswiet J. Analysis of surface roughness for parts formed by computer numerical controlled incremental forming. *Proc Inst Mech Eng Part B J Eng Manuf.* 2004;218(10):1307-1312.
- [16] Allan K, Hamilton S. *Friction and external surface roughness in Single Point Incremental Forming: A Study of Surface Friction, Contact Area and the "orange Peel" Effect.*; 2010.
- [17] Oraon M. Statistical analysis to predict the surface roughness in single point incremental forming of Cu67Zn33 alloy. *Int J Product Qual Manag.* 2020;31(4):593.
- [18] Hamilton K, Jeswiet J. Single point incremental forming at high feed rates and rotational speeds: Surface and structural consequences. *CIRP Ann.* 2010;59(1):311-314.
- [19] Durante M, Formisano A, Langella A. Comparison between analytical and experimental roughness values of components created by incremental forming. *J Mater Process Technol.* 2010;210(14):1934-1941.
- [20] Oleksik V, Pascu A, Deac C, Fleacă R, Bologa O, Racz G. Experimental study on the surface quality of the medical implants obtained by single point incremental forming. *Int J Mater Form.* 2010;3(SUPPL. 1):935-938.
- [21] Ham M, Jeswiet J. Single Point Incremental Forming Limits Using a Box-behnken Design of Experiment. *Key Eng Mater.* 2007;344:629-636.
- [22] Abd Ali R, Chen W, Al-Furjan MSH, Jin X, Wang Z. Experimental Investigation and Optimal Prediction of Maximum Forming Angle and Surface Roughness of an Al/SUS Bimetal Sheet in an Incremental Forming Process Using Machine Learning. *Materials (Basel).* 2019;12(24):4150.
- [23] Liu Z, Liu S, Li Y, Meehan PA. Modeling and Optimization of Surface Roughness in Incremental Sheet Forming using a Multi-objective Function. *Mater Manuf Process.* 2014;29(7):808-818.
- [24] Phadke MS. *Quality Engineering Using Robust Design.* Prentice Hall PTR <https://dl.acm.org/doi/abs/10.5555/525794>
- [25] Jeyapaul R, Shahabudeen P, Krishnaiah K. Quality management research by considering multi-response problems in the Taguchi method - A review. *Int J Adv Manuf Technol.* 2005;26(11-12):1331-1337.
- [26] Kecman V. *Learning and Soft Computing: Support Vector Machines, Neural Networks, and Fuzzy Logic Models.* MIT press; 2001.
- [27] Oraon M, Sharma V. Prediction of surface roughness in single point incremental forming of AA3003-O alloy using artificial neural network. *Int J Mater Eng Innov.* 2018;9(1):1-19.
- [28] Liew KM, Tan H, Ray T, Tan MJ. Optimal process design of sheet metal forming for minimum springback via an integrated neural network evolutionary algorithm. *Struct Multidiscip Optim.* 2004;26(3-4):284-294.

- [29] Mulay A, Ben S, Ismail S. Artificial Neural Network Modeling of Quality Prediction of a Single Point Incremental Sheet Forming Process. 2017;(June 2018):244-250.
- [30] Harfoush A, Haapala KR, Tabei A. Application of artificial intelligence in incremental sheet metal forming: A review. *Procedia Manuf.* 2021;53(2020):606-617.
- [31] Oraon M, Sharma V. Application of artificial neural network: A case of single point incremental forming (SPIF) of Cu67Zn33 alloy. *Manag Prod Eng Rev.* 2021;12(1):17-23.
- [32] Pepelnjak T, Sevšek L, Lužanin O, Milutinović M. Finite Element Simplifications and Simulation Reliability in Single Point Incremental Forming. *Materials (Basel).* 2022;15(10):3707.